Stick-slip instability for viscous fingering in a gel

N. Puff, G. Debregeas, J.-M. Di Meglio, D Higgins, D. Bonn, C. Wagner

Stick-slip instability for viscous fingering in a gel

N. Puff, G. Debrégeas, J.-M. di Meglio(*), D. Higgins ([1]),
D. Bonn and C. Wagner ([2])

[1] *Institut Charles Sadron (CNRS UPR22), 6 rue Boussingault, 67083 Strasbourg Cedex, France*

[2] *Laboratoire de Physique Statistique (CNRS UMR 8550), École Normale Supérieure, 24 rue Lhomond, 75231 Paris Cedex 05, France*

PACS. 47.50.+d – Non-Newtonian fluid flows.
PACS. 82.70.Gg – Gels and sols.
PACS. 83.60.Wc – Flow instabilities.

Abstract. – The growth dynamics of an air finger injected in a visco-elastic gel (a PVA/borax aqueous solution) is studied in a linear Hele-Shaw cell. Besides the standard Saffmann-Taylor instability, we observe - with increasing finger velocities - the existence of two new regimes: (a) a stick-slip regime for which the finger tip velocity oscillates between 2 different values, producing local pinching of the finger at regular intervals, (b) a "tadpole" regime where a fracture-type propagation is observed. A scaling argument is proposed to interpret the dependence of the stick-slip frequency with the measured rheological properties of the gel.

Introduction. – When a fluid is injected into a more viscous liquid, the invading front is unstable at early stages and splits into multiple fingers. This process, known as the Saffmann-Taylor (ST) problem [1], has been extensively studied as a simple example of non-linear dynamical instability. The width of the fingers arises from a competition between the surface tension, which tends to widen them, and the viscous stress, which tends to make them thinner. In a standard ST experiment, the fluids are confined between two parallel plates separated by a gap of thickness b much smaller than any other length scale. For air driven into a Newtonian liquid, the stationary width w of the fingers relative to the gap thickness b only depends on the capillary number $Ca = \eta U/\gamma$ where η is the liquid viscosity, U the bubble tip velocity and γ the liquid surface tension. When the bubble is forced to grow in a linear channel of width $W << b$, the ratio w/W decreases as Ca is increased until it reaches a limiting value equal to one-half.

In most practical situations however, the liquid phase (typically polymer solutions or complex multi-phase systems) does not show a purely Newtonian rheology. Many experimental and theoretical studies have thus attempted to understand the modifications of the ST results associated with more complicated rheological characteristics of the invaded phase [2–4]. Two situations may be distinguished. For liquids with shear rate dependent viscosity, the shape of the finger is slightly modified. This can be understood by considering the inhomogeneous

(*) Université Louis Pasteur and Institut Universitaire de France

shearing experienced by the liquid across the channel : the shear rate in the central part (of order $\dot{\gamma} \sim U/b$ with b being the plate spacing of the Hele-Shaw cell) is higher than on the sides. Hence, a bubble penetrating a shear-thinning liquid for instance tends to be thinner than what is expected for a Newtonian liquid because the central part of the channel offers less resistance to the flow [5,6]. For strongly elastic liquids, a richer variety of situations is observed because elastic stresses can develop in the liquid phase and affect the bubble growth. This internal stress generally enhances tip splitting or even leads to fracture formation, yielding highly ramified patterns [2, 7, 8].

Here we study the rapid penetration of a gas into a visco-elastic gel which exhibits a plateau in the stress/strain rate curve. Three different tip dynamics are evidenced. A low velocity regime where the bubble shape remains very similar to the standard ST process. A high velocity regime where the bubble assumes a tadpole profile. In between this regime, we observe a stick-slip transition regime where the bubble tip velocity oscillates between two different values. Stick to slip transitions are found to occur at regular spatial intervals and produce local pinchings of the finger.

Experiments. – We have used aqueous solutions of PVA/Borax as model visco-elastic gels. PVA (poly(vinyl alcohol)) has been purchased from Prolabo (Rhodoviol 30/5) and borax (sodium tetraborate decahydrate) from Aldrich. We have followed the preparation method described by Garlick [9]. The visco-elasticity of this solution arises from temporal cross-linkings of the PVA chains through H-bonding with the borax groups. The concentration of PVA in water was fixed and equal to 3 % (weight/weight) while the concentration of borax has been changed between 0.125 and 5 % (w/w) in order to vary the rheological properties.

The Hele-Shaw is made of two rectangular plastic (PMMA) plates of thickness 1.25 cm, tightened together by 12 screws. The two plates are separated by a thin Teflon sheet of uniform thickness b. This spacer is U-shaped to define a one-end open channel of width W and length $L = 20$ cm filled with the gel. In most experiments, the distance b and W are respectively 1 and 5 mm (in a few experiments, W and b have been changed to check for geometrical constraints effects). A 1 mm hole is drilled in the lower plate to allow for the air injection. The air is supplied by a 25 ml syringe at constant pressure P measured by a gauge in derivation. A bright background is placed below the cell to give a good contrast on the bubble edge. Images are captured in the central part of the set-up to avoid end effects with a high speed video camera (Kodak Motion Corder). Subsequent tracking of the bubble tip is performed using an image analysis software (IDL) to produce growth velocity sequences $U(t)$. In the standard ST regime, the tip velocity U is proportional to the applied pressure gradient $(P - P_0)/x$ where x is the distance to the outlet and P_0 the external pressure. In a single experiment, we therefore explore a large range of velocities U. We furthermore vary $(P - P_0)$ (around 1 atmosphere) to access a wider dynamical range.

Results. – At low velocity, the bubble grows smoothly with a velocity U increasing as the inverse of the distance to the outlet. The width w of the bubble however is found to be slightly below the value $W/2$ expected for a Newtonian liquid. For a certain threshold velocity (of the order of a few mm.s^{-1}), the bubble experiences a sudden bulging (see Fig. 1A). The tip hops rapidly ahead, with a significant decrease of its radius of curvature. In about 30 ms, the velocity increases by a factor of 10 to 20. The velocity then rapidly recovers its initial value as the bubble front relaxes to its initial shape, leaving a pinch, a narrow section of the finger behind (Fig. 1A). We also observe, with the bright background illumination, that the shape of the bubble at the onset of bulging remains visible after the tip has moved ahead. This indicates that the deposited liquid film thickness is strongly modified at this position: the pinching also occurs in the vertical direction.

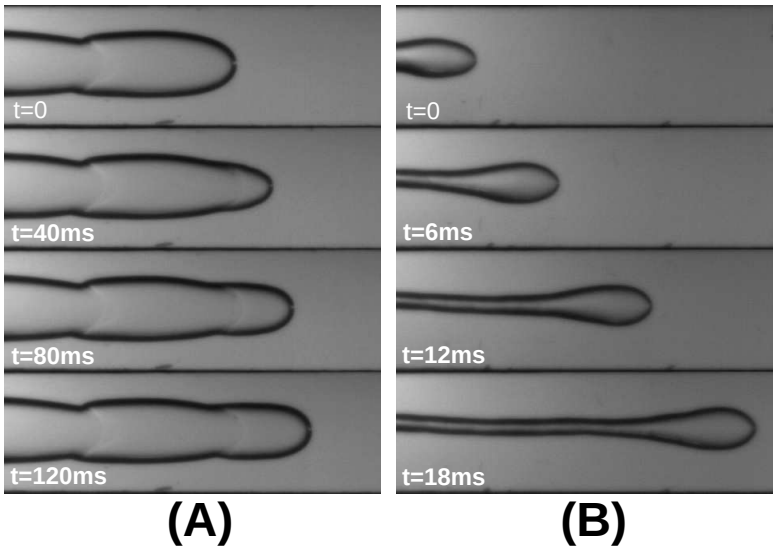

Fig. 1 – Sequences of growth showing the two new regimes. The width W and depth b of the channel are respectively 5 and 1 mm. (A): Stick-slip regime. After bulging, the deposited film is thicker: the shape of the bubble in the first image can therefore be detected on the following snapshots. (B): The rapid "tadpole" regime.

Once the first bulging is triggered, we observe up to fifteen other events occurring at regular distances λ (Figure 2). Figure 2B shows the different values of λ for different gels as a function of the time interval Δt between the 2 successive bulges. Each experiment provides several measurements of λ over a certain range of Δt. This range is then extended by varying the applied pressure, yielding the large number of data points. For a given gel, λ appears to be independent of Δt, or equivalently of the tip velocity at the onset of bulging. However, λ decreases as the borax volume fraction is increased.

In all experiments, the last bulge is followed by a transition to a regime of rapid bubble growth (see Fig. 1A): instead of recovering its original velocity and shape, the tip keeps accelerating and the bubble assumes a tadpole shape, characterized by a rounded head and a thin cylindrical tail (of diameter smaller than the gap b).

Rheology. – To characterize the visco-elastic properties of the gels, several standard rheological measurements have been performed. The rheometer in use was a Reologica Stresstech with cone and plate geometry (diameter 40 mm, angle 4°). These measurements were checked against those in a Couette cell: no significant differences between the two geometries were observed, validating the results.

The rheometer was operated in controlled shear rate mode. Figure 3 shows the shear stress σ as a function of the shear rate $\dot{\gamma}$ for three different samples. At lower shear rates, the stress increases linearly with the shear rate yielding a constant viscosity $\eta = \sigma/\dot{\gamma}$. Above a certain shear rate, the gels undergo a slight shear thickening. This is illustrated by a linear fit taken to the low shear rates data for the 0.25 % w/w borax sample in Figure 3. The viscosity increase is of the order of several percents.

Upon further increasing the shear rate, a stress plateau *i.e.* a constant stress σ_p over a range of shear rates is observed. After the plateau, the stress increases again with the shear rate but the viscosity remains shear-thinning. For even higher shear rates, secondary flow

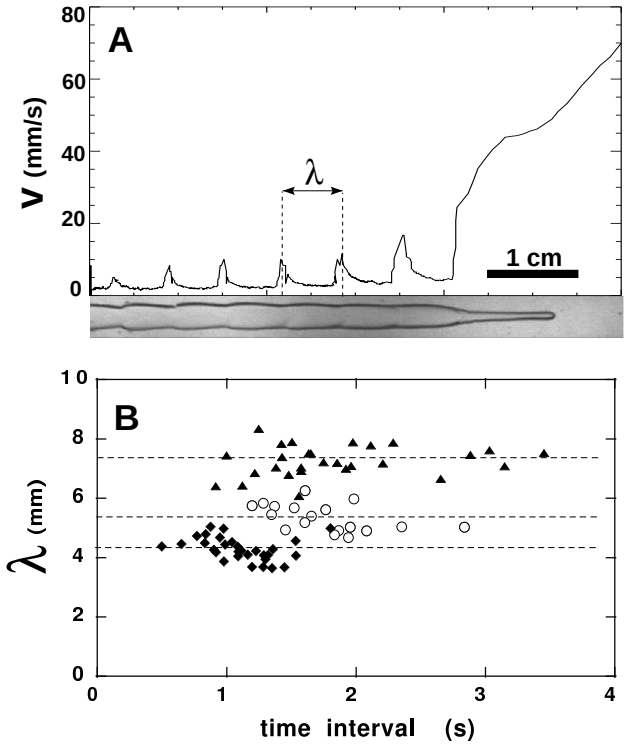

Fig. 2 – Periodicity of the bulgings in the stick slip regime. (A) Tip velocity as a function of its position in the channel (the snapshot corresponds to the bubble shape after the end of the stick-slip regime). Each bulging is associated with an overshoot of the tip velocity. The maxima are used to evaluate the stick-slip wavelength. The last bulge is followed by the "tadpole" regime where the tip velocity rapidly increases. (B) Different measurements of the stick-slip wavelength as a function of the time interval between the two tip velocity overshoots. Each set of data corresponds to a different gel (Borax concentration are respectively ▲: 0.125 %, ○: 1 %, ♦: 2 %). For each gel, the stick-slip wavelength is independent of the time interval between bulgings.

instabilities due to the normal stresses, *e. g.* the Weissenberg effect in the Taylor Couette cell, become significant and the liquid expels itself from the measurement cell.

Discussion. – The observation of a stress plateau is surprising: it indicates that for a given stress σ_p, different shear rates, and consequently different viscosities exist in one and the same system. As this is unlikely to happen for our material, the most natural interpretation would be that, instead of two viscosities, there are two possible boundary conditions. This effect is known as *stick-slip* behaviour and has frequently been associated with the occurrence of stress plateaus in the engineering literature. In agreement with the occurrence of stick-slip, we find that the measured viscosity oscillates with a large amplitude in the vicinity of the plateau stress. This suggests that the oscillations observed for the fingers are also due to a stick-slip motion. Consistently, we observe that the critical tip velocity U_c for the onset of the instability in the ST experiments corresponds to a typical shear rate ($\sim U_c/b$) of the order $1s^{-1}$, which decreases with increasing borax concentration. This shear rate value is thus compatible with the critical shear rate for the occurrence of the stress plateau in the rheology measurements for the different gels (Figure 3). In order to further test this hypothesis, we

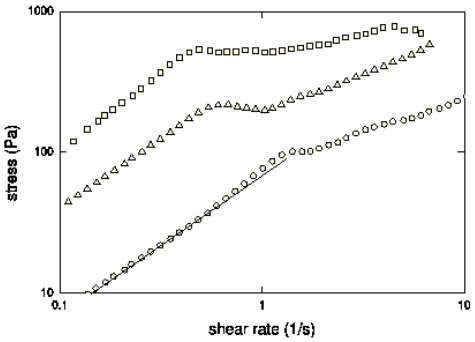

Fig. 3

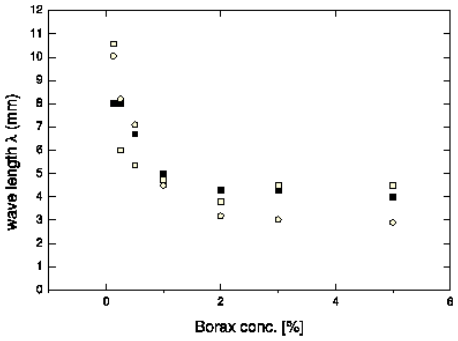

Fig. 4

Fig. 3 – Shear stress σ as a function of the shear rate γ for different borax concentrations. ○: 0.25 %, △: 0.5 %, □: 1 %. The straight line is the extrapolated linear fit of the 0.25 % borax data at shear rates $\gamma < 0.5$ s^{-1}.

Fig. 4 – Stick-slip wavelength λ from: (■) the ST experiment, calculated with equation 1 using the plateau stress σ_p (○) or the elastic modulus G_0 deduced from the oscillatory measurements (□). The numerical prefactor is found to be equal to 17 for the two estimations.

compare the observed wavelength of the oscillating fingers with the results of a linear stability analysis for visco-elastic fingering.

Recent theory and experiments [4] on the instability in visco-elastic (yield stress) fluids has shown that a linear stability analysis of the flat interface can be performed; the wavelength of maximum growth follows as: $\lambda = \sqrt{\gamma b/\sigma_w}$, with σ_w the wall shear stress, γ the surface tension and b the plate spacing of the Hele-Shaw cell. For yield stress fluids, it was demonstrated that the wavelength at early times after the instability verifies this prediction with the wall shear stress equal to the yield stress plateau. In a similar way, for our visco-elastic fluid, the wall shear stress in the stick-slip regime should be given by the plateau value σ_p. Under this assumption, one would then expect the oscillation wavelength λ to write:

$$\lambda = \sqrt{\gamma b/\sigma_p} \tag{1}$$

This has a number of interesting consequences. First, it explains why the characteristic wavelength turns out to be independent of the velocity. The other consequences are that the finger width should scale as the square root of the plate spacing and be independent of the channel width. We actually observed that doubling the depth b of the channel increases λ by a factor of about 1.15 (instead of the expected ~ 1.4). However, a similar increase was found when doubling the width W of the channel. In this geometry with a low W/b ratio, the lateral confinement also plays a significant role in selecting the oscillation wavelength.

Figure 4 compares this prediction of λ (expression (1)) to the experimentally observed oscillation wavelength. We find a similar dependence of both data on the plateau stress σ_p obtained from rheology measurements; if we use the surface tension of water (72 mN.m^{-1}) as the surface tension of our aqueous polymeric fluid, the proportionality constant is found to be equal to 17.

That the physical origin of the instability is elastic follows directly if we determine the elastic modulus from rheology measurements in oscillation mode. The measurements indicate that the system has more than a single relaxation time [11]. We therefore determine the

elastic modulus G_0 as the point where the storage modulus G' equals the loss modulus G''; this is exact for a Maxwell fluid, and should be a good approximation for our fluid. From these experiments it follows that the elastic modulus G_0 and the plateau stress are indistinguishable within the experimental error. Therefore, we obtain an equally good description of the data in Fig. 4 when plotting $\lambda = \sqrt{\gamma b/G_0}$, with the same proportionality constant.

Beyond the oscillating regime, the onset of the tadpole regime can be understood as a transition to a "soft fracture" dynamics. This regime appears to be qualitatively very different from the viscous one. In standard ST experiment, the injected air displaces a large volume of liquid, inducing dissipation in the whole region ahead of the tip. By contrast, in this fast regime, the total flux of liquid becomes extremely small and the viscous dissipation is confined to a very small volume around the tip (as probed by the absence of motion of air bubbles or dust that can be trapped between the tip and the outlet). If we evaluate the typical time-scale τ_p for the passage of the head (its length divided by the tip velocity) we find $\tau_p << \tau_r$ where $\tau_r \sim 1s$ is the relaxation time of the gel deduced from rheology measurements. Therefore, most of the gel experiences an elastic deformation which is mainly recovered after the tip has moved by. It is therefore qualitatively similar to a fracture type dynamics. The unusual rounded shape of the tip is due to the low value of the elastic modulus G_0 for this material (of order $100-500Pa$). By comparing elastic to surface forces, one can access a typical lengthscale $h_0 = \gamma/G_0$ for the curvature of the tip of order $1mm$. This value is consistent with values measured in the experiments.

Conclusion. – In conclusion, we have observed an oscillating growth dynamics occurring upon injection of an air bubble into a visco-elastic gel. This result is qualitatively different from what had been observed so far in ST experiments with non-Newtonian liquids. By contrast with other systems where the elastic characteristic of the invaded phase was found to increase tip splitting [8], here the finger experiences an instability along its growth direction. As a result, the thickness of the deposited film exhibits strong but spatially regular modulations.

Apart from geometrical parameters, we found the oscillation wavelength to be entirely controlled by the visco-elastic property of the gel, and to be independent of the injection rate. We think that this observation may be helpful, for instance, to understand the shear-induced emulsification of a dispersion of inviscid droplets in a visco-elastic matrix: it has been found that such a combination could lead to very monodisperse emulsions [12]. The final droplets size could result from a similar process occurring during the rapid elongation of the drops in the visco-elastic phase.

* * *

We would like to thank J. Meunier, P. Sens and J.F. Joanny for fruitful discussions. LPS de l'ENS is UMR 8550 of the CNRS, associated with the Universities Paris 6 and 7.

* * *

REFERENCES

[1] P.G. Saffman and G.I. Taylor, *Proc. R. Soc. London, Ser. A*, **245** (1958) 312
[2] K.V. McCloud and J.V. Maher, *Physics Reports*, **260** (1995) 260139
[3] P. Coussot, *J. Fluid Mech.*, **380** (1999) 363
[4] A. Lindner, P. Coussot and D. Bonn, *Phys. Rev. Lett.*, **85** (2000) 314

[5] A. Lindner, D. Bonn and J. Meunier, *Physics of Fluids*, **12** (2000) 256
[6] L. Kondic, M. Shelley and P. Pallfy-Muhoray, *Phys. Rev. Lett.*, **80** (1998) 1433
[7] H. Zhao and J. V. Maher, *Phys. Rev. E*, **47** (1993) 4278
[8] D. H. Vlad and J. V. Maher, *Phys. Rev. E*, **61** (2000) 5439
[9] M. Garlick, http://www.delta.edu/slime/slime.html
[10] Yuan Chen Chung and Tzyy-Lung Yu, *Polymer*, **38** (1997) 2019
[11] I.D. Robb and J.B.A.F. Smeulders, *Polymer*, **38** (1997) 2165
[12] T. G. Mason and J. Bibette, *Phys. Rev. Lett.*, **77** (1996) 3481